A comparison of SWCA for TMSC and cellulose films is presented in Figure 1.1. SWCA of a typical TMSC film is 98.0 ± 2.8 °, of a cellulose film 25.0 ± 0.6 °, meaning that the hydrophilicity was increased after acidic hydrolysis of the silylether groups, indicating that the cellulose film was regenerated.

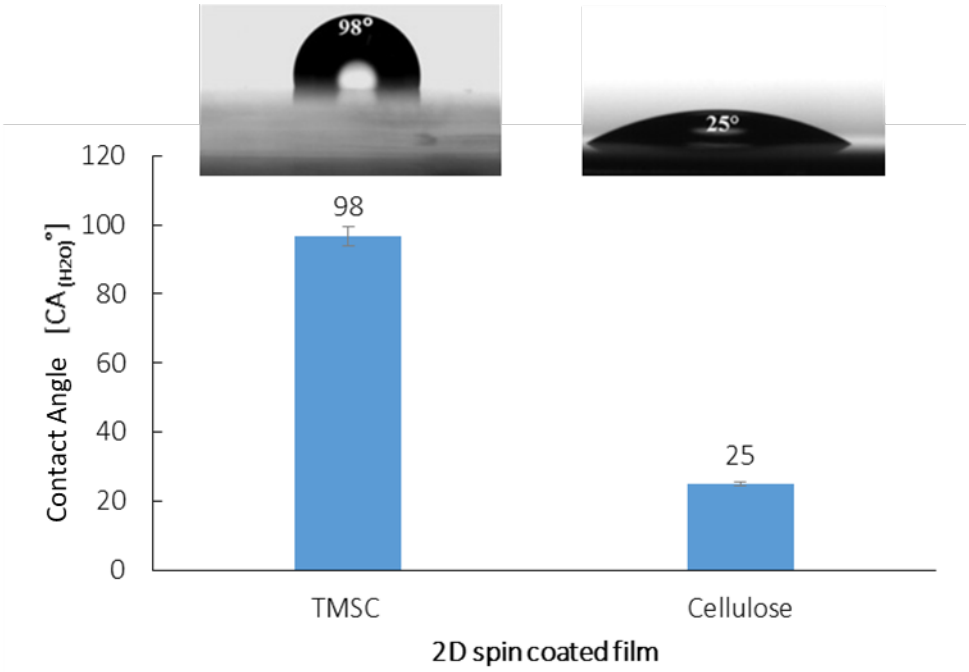

Static Water Contact Angles (SWCA) on TMSC and regenerated cellulose films.

Characterisation of polymer solutions: The addition of BCG into the CA electrospinning solution (17 wt% CA; 85% AcOH) should not influence the solution's viscosity, conductivity and surface tension, and it should not hinder the electrospinning process.

Electrospinning process: The optimal spinning procedure should be as follows: Voltage: 75 kV, Electrode distance: 160 mm, electrode rotation speed: 3.8 rpm, ambient humidity: 30%, ambient temperature: 20°C and electrospinning time: 40 min.

Characterisation of electrospun mats: Figure 1.2 a) shows the electrospun mats before and after immersion in solutions with different pH. From Figure 3.3 a) it can be observed that the CA nanofibrous mats with incorporated BCG (Figure 1.2 a)– before) is slightly yellow just after the electrospinning process, caused by the acidic conditions during fibre formation (acetic acid). The colour of the electrospun mat with included BCG and dipped in both acidic solutions (pH 2 and 4), where BCG occurs in its protonated form (see Figure 3.2), is intense yellow (Figure 1.2 a) – after). The colour of the sample immersed into alkaline solutions (pH 9 and 10, non-protonated BCG) is blue. The green colour of the sample at pH 7 is due to the fact that both species (protonated and non-protonanted BCG) are present in such quantities that the observed colour originates from a combination of yellow and blue.

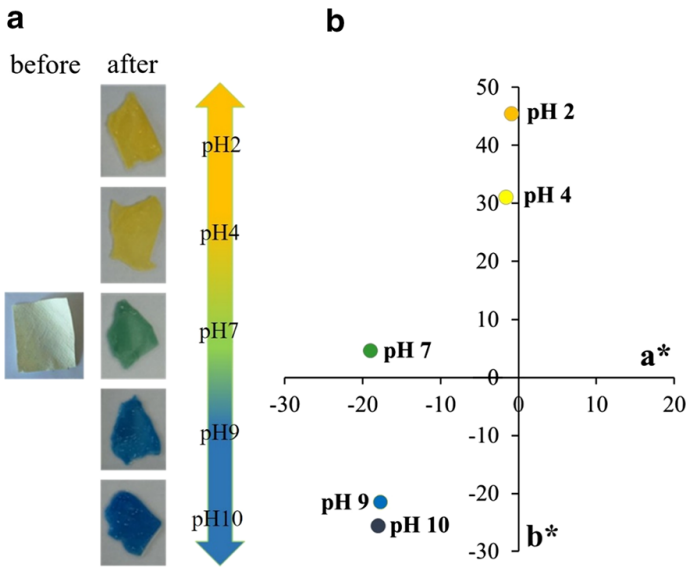

The coloured nanofibres depending on the solutions' pH: a) Samples' photographs before and after immersion in pH solutions; b) Position of samples in the CIE a*–b* plane.

The results from the colour measurements and colour coordinates (CIE L*a*b*) for the samples immersed at different pH values (2, 4, 7, 9 and 10) are depicted in Fig. 1.2 b). From Figure 1.2 b) it can be seen that, after the immersion of the electrospun mat in acidic pH, the lower the pH of solution is, the more intensive is the yellow colour of electrospun mat, while, at the same time, the blue colour lost its intensity (higher b* value); and vice versa, after immersion of electrospun mat in alkaline pH, the higher the pH of solution is, the lower is the obtained b*value. The neutral solution (pH 7) led to a green hue of the sample, i.e. a* is - 18.94 and b* is 4.51, although the dye producer declares that the BCG solution has a visual transition interval (green colour) at lower pH values (3.8–5.4). It should be kept in mind that the halochromic behaviour of the BCG in the surrounding CA matrix altered compared to its behaviour in solution, which is most likely attributed to the dye-polymer interactions [46], as well as the different accessibility of the dye molecules in the nanofibrous materials (compared to its molecular dispersion).

Figure 1.3 a) shows the absorbance spectra of BCG in buffers with pH 4 (yellow) and pH 9 (blue). The acid and basic forms of BCG have an isosbestic point in their UV-Visible spectrum, around 540 nm, indicating that the two forms interconvert directly without forming any other substance. Figure 1.3 b) shows the electrospun mat after two cycles of immersion in buffer solutions with pH 9 and 4. The colour of the electrospun mat after dipping in buffer solution with pH 9 is blue. Then, the sample was transferred to buffer solution with pH 4, and the colour was changed to yellow. Then, the sample was transferred again in buffer solution with pH 9, and the colour changed to blue with the same intensity as in the first cycle. After immersion in buffer solution with pH 4 in the second cycle, the colour changed again to yellow with the same intensity as in the first cycle.

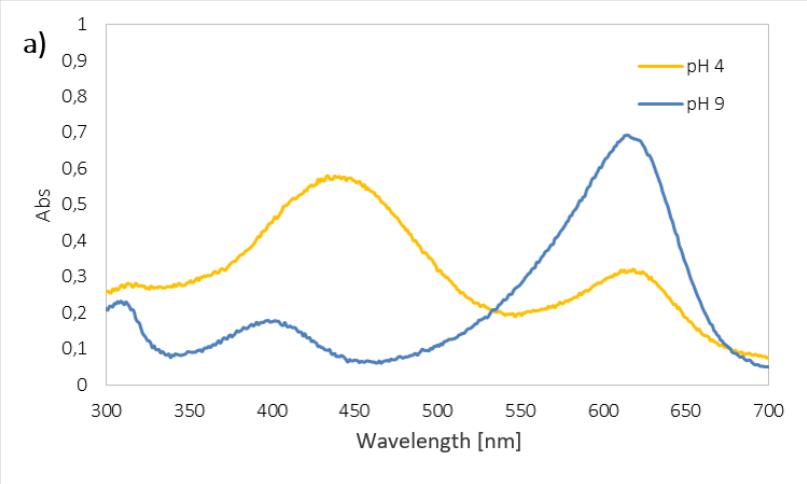

a) UV-Vis spectra of BCG in buffers with pH 4 (yellow) and pH 9 (blue), b) The electrospun mat after two cycles of immersion in buffer solutions with pH 9 and 4.

The leaching test showed that the concentration of BCG in buffers was below the detection limit, since no peak was detected in the wavelength from 200 to 800 nm.

Microscopy analysis: Figure 1.4 shows the results obtained from the optical microscopy measurements of 3D printed scaffolds using NFC-CMC-CitricA-SHP-AKD at different printing pressures. The microscopy images for samples printed at different pressures are shown in the left side. The pore sizes calculated from the images are given on the right side. Results show that the pore size of the printed structures can be tuned by simply tuning the pressure. A higher pore size is observed at lower pressure (160 kPa). At 200 kPa, no pores are detected due to closing of the print.

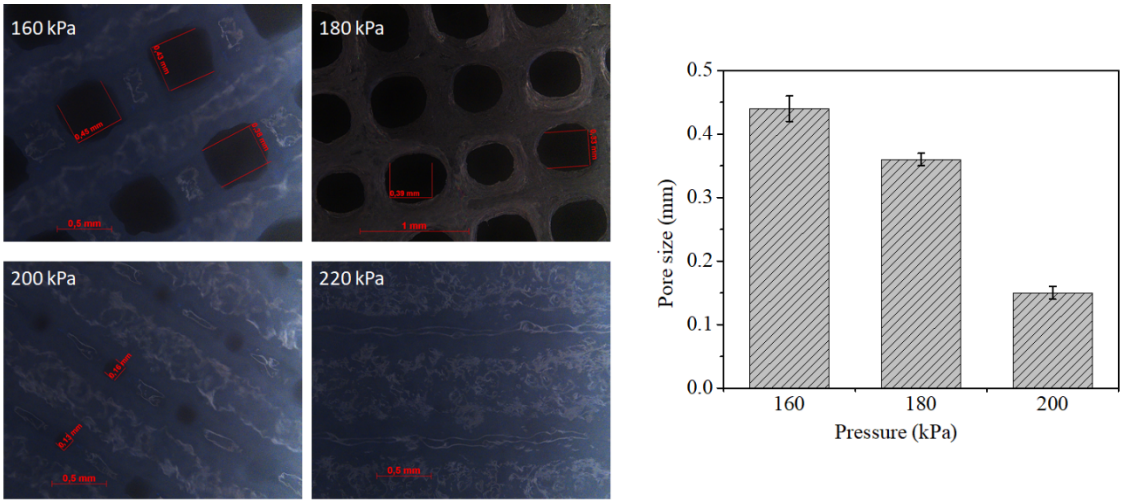

Left side – microscopy images and pore size of the 3D printed structures.

Wettability: Figure 1.5 (a) shows the surface of pure cellulose material (casted and lyophilised NFC) immediately after deposition of a water drop on the surface of the material. One can observe that the water drop is absorbed into the material immediately, meaning that the material is hydrophilic. Figure 1.5 (b) shows the surface of a 3D printed sample (NFC-CMC-CitricA-SHP-AKD after heat curing) after the placement of three water drops on the surface of the material. The drops are not absorbed into the material, meaning that the material is hydrophobic.

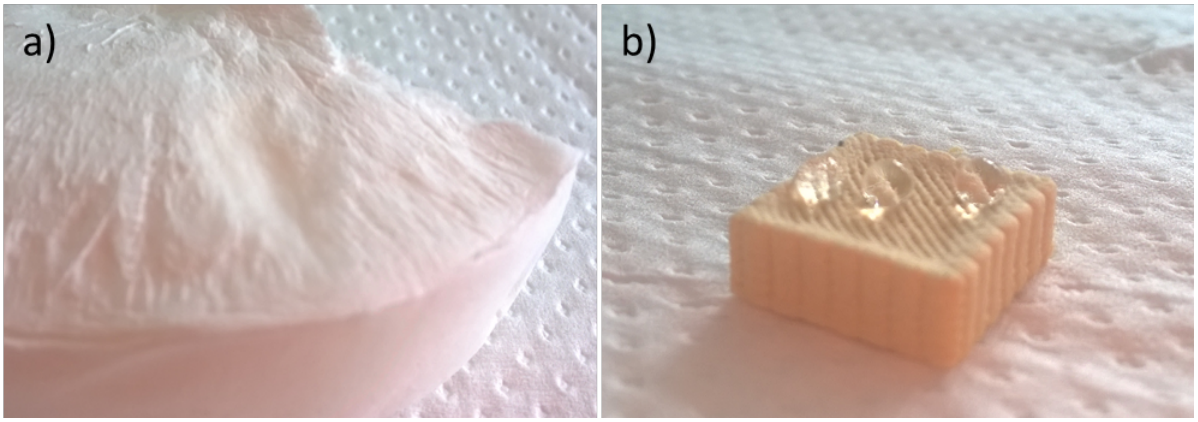

Hydrophilic pure cellulose material (a); hydrophobic 3D printed flame retardant material (b).

Flammability test: Figure 1.6 (a) shows the pure cellulose material (casted and lyophilised NFC) which burns fast by spreading the flame over the whole material after removal of the ignition source. Figures 1.6 (b and c) show the flame retardant 3D printed material, where the fire is extinguished after the ignition source is removed.

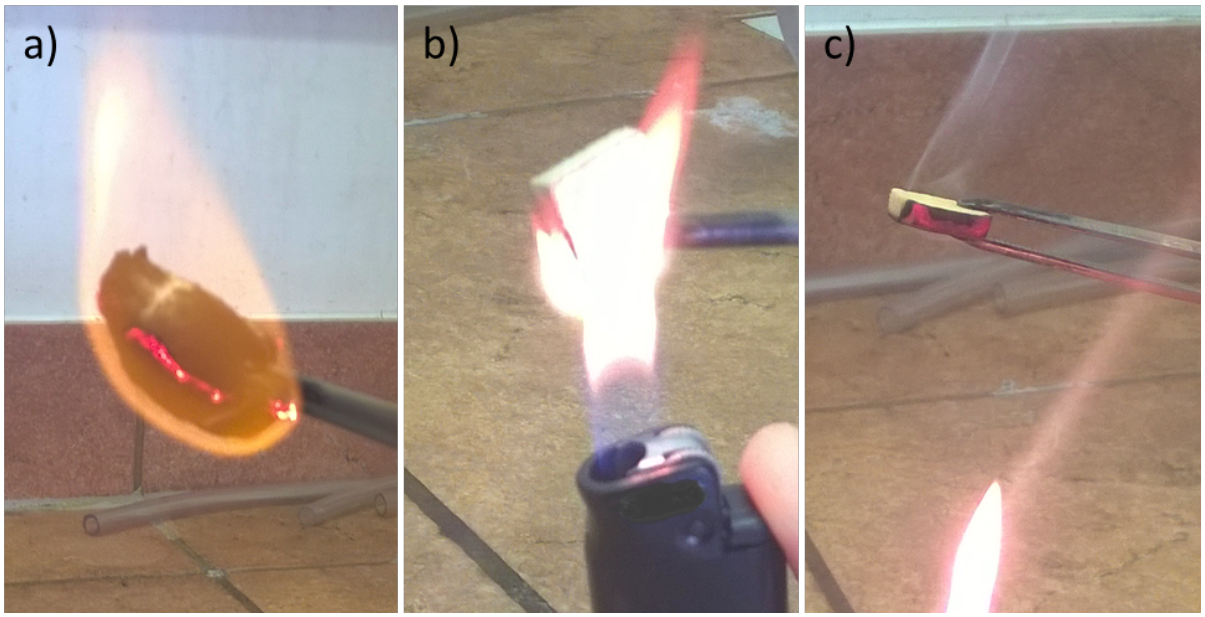

Flammable pure cellulose material (a); flame retardant 3D printed material (b and c).